Chapter 5
Design of FOPID controller using modified grey wolf optimization

5.1 Introduction

The most complicated assignment for any meta-heuristic technique is to offer a smooth equilibrium between exploration and exploitation [174]. After thorough analysis of the outcomes of GWO-algorithm, it is concluded that in some cases it is trapped into local optima [175]. Hence, some possible amendment is needed to get more refine and best global solution while designing the FOPID controller. In this chapter a modified version of GWO-algorithm (i.e. MGWO-algorithm) is presented for optimization of parameters of the FOPID controller.

5.2 Modified Grey Wolf Optimizer (MGWO)

Trapping of solution in local optima happens only due to the dependency of the GWO-algorithm upon two coefficients i.e. 'A' and 'C' as discussed in section 4.3 [169], [171], [173]. Hence, a novel position updating technique is desired to avoid the situation of stucking in local optima.

Here, a novel approach is proposed for updating the position of wolves. The approach maintains a better balance between exploration and exploitation to produce the optimum solution in entire search space. The positions of the wolves are updated through basic concept of mathematics. Leader of the wolves i.e. Alpha is responsible for exploitation and gives the best solution among all. Rest of the wolves are liable for exploration. Major modifications in the different hunting steps of the MGWO is in its mathematical model discussed in subsection ahead.

5.2.1 Modification in encircling process

Encircling of the prey by wolves in MGWO requires the following mathematical equations.

$$\vec{D} = \vec{C}\vec{X}_P(t) - \vec{X}(t).U(-2a, 2a) \tag{5.1}$$

$$\vec{X}(t+1) = \vec{X}(t).\vec{A}.U(-2a, 2a) \tag{5.2}$$

In Equations 5.1 and 5.2 a new the term $\mathrm{U}(-2\mathrm{a}, 2\mathrm{a})$ is added as compared to Equation 4.1 and 4.2. The term $\mathrm{U}(-2\mathrm{a}, 2\mathrm{a})$ gives a uniformly distributed random number in the interval $[-2, 2]$. In the proposed approach exploitation and exploration depends on the value of the term $\mathrm{U}(-2\mathrm{a}, 2\mathrm{a})$. Exploitation occurs if $\mathrm{U}(-2\mathrm{a}, 2\mathrm{a})$ gives a number closer to 1 otherwise, exploration occurs. Calculation of coefficients 'A' and 'C' is done in same manner as in Equations 4.3 and 4.4 respectively in the previous chapter.

5.2.2 Selection of leader

Selection of the leader i.e. best wolf Alpha is based on its fitness value. The positions of the wolves are updated according to the best fitness value computed as shown in Equation 5.3.

$$\vec{X}(t+1) = \begin{cases} \vec{X}(t).\vec{A}.U(-2a, 2a), & fitness\{\vec{X}(t+1)\} < fitness\{\vec{X}(t)\} \\ \vec{X}(t) & otherwise \end{cases} \tag{5.3}$$

Equation 5.3 confirm that the next position of the wolves in MGWO-algorithm depend only on the value of variable $'A'$ but it also depend on the new variable $U(-2a, 2a)$.

Apart from these changes in the algorithm a novel fitness function is defined to get the fittest value of the FOPID controller parameters using MGWO.

5.2.3 A novel fitness function

The fitness function defined in the present work is the weighted sum of rise-time (RT), settling-time (ST), peak-overshoot (MP), Gain-Margin (GM), Phase-Margin (PM), integral time weighted absolute error ($ITAE$) and integral time weighted square error ($ITSE$). The expression of fitness function is given as:

$$J = \frac{(ITAE + ITSE) * \mathrm{w}_1 + (\mathrm{RT} + \mathrm{ST} + MP) * \mathrm{w}_2}{(GM + PM) w_3} \tag{5.4}$$

where $w_1, w_2,$ and w_3 are the weighting factors. Selection of w_i is tricky and is obtained trial & error.

In this work, the weighting factors are chosen according to their percentage of contribution for the desired result. Numerical values of weights considered are 0.5, 15 and 10 respectively. The fitness function is used for optimization of FOPID parameters using MGWO-algorithm for each of the problem elaborated ahead. Because of having time-domain characteristics in numerator and frequency domain characteristic in denominator of the fitness function, it provide a proper balance between both the characteristics of the system.

The flowchart and pseudo code of the MGWO-algorithm are shown in Figure 5.1 and Figure 5.2 respectively.

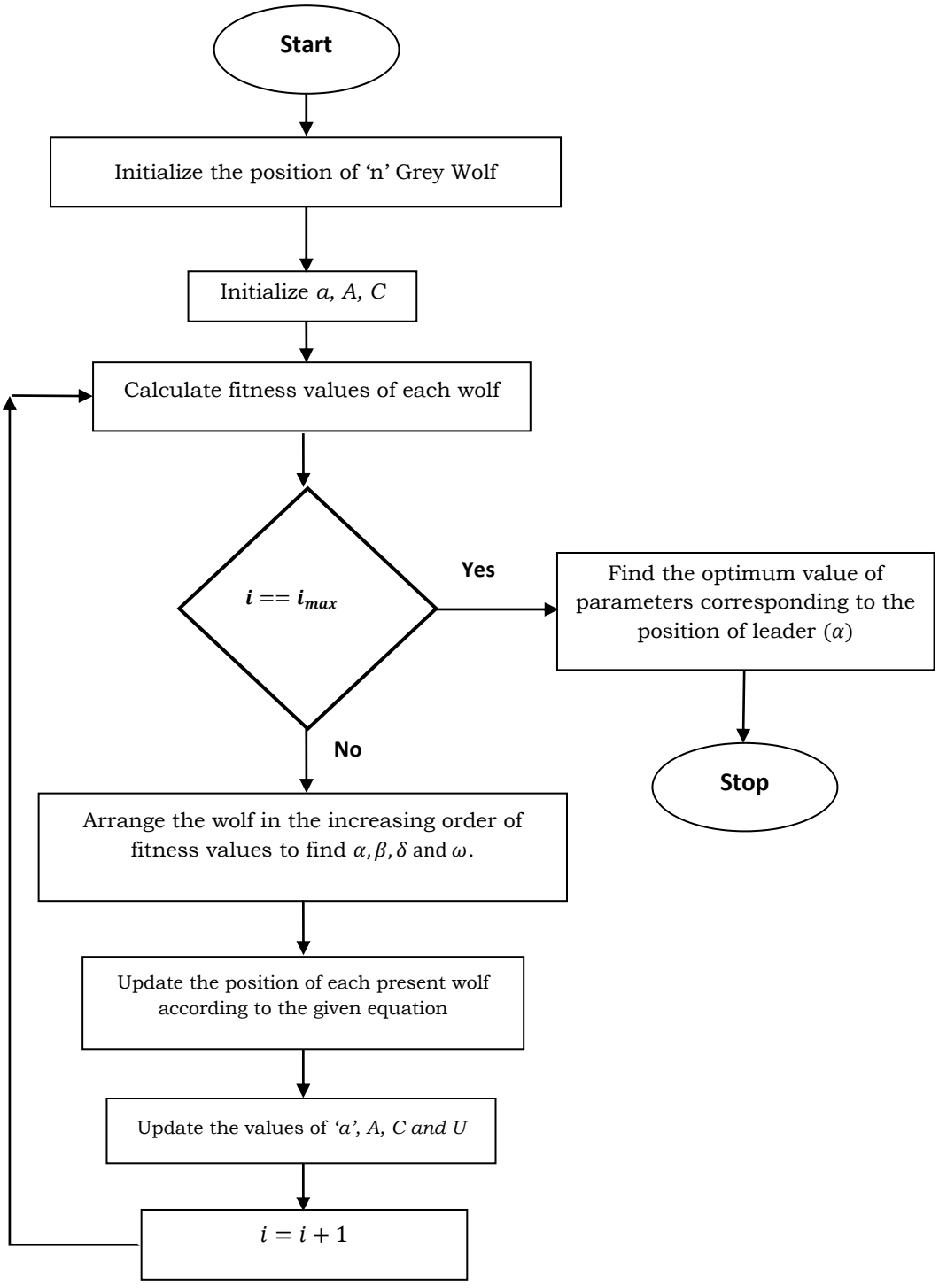

Fig. 5.1. Flowchart of MGWO-algorithm

Initialize the grey wolf population $X_i(i = 1,2 \ldots . . n)$
Initialize a, A, C, U
Calculate the fitness of each search agent
$X_\alpha = the\ best\ search\ agent$
$X_\beta = the\ second\ best\ search\ agent$
$X_\delta = the\ third\ best\ search\ agent$
While ($t <$ *Max. number of iterations*)
    for *each search agent*
        Update the position of the current search agent by equation (5.3)
    end for
    Update a, A, C, U
    Calculate the fitness of all the search agents
    Update $X_\alpha, X_\beta, X_\delta$
    $t = t + 1$
end while
return X_α

Fig. 5.2. Pseudo code of the MGWO-algorithm

Now, the concept of MGWO-algorithm discussed above is implemented here to design the FOPID controller for all the cases discussed in the chapter 3. Again, the best result is considered after 100 iterations in every case of optimization. Performance of FOPID controller optimized using MGWO-algorithm for various systems is discussed below.

5.3 Illustrative Examples

5.3.1 Design of an FOPID controller for third order linear plant

The third order linear system in section 3.3.1 is again considered to validate the effectiveness of the algorithm. The optimized value of the parameters of FOPID controller using MGWO-algorithm (i.e. MGWO-FOPID) are obtained as: $K_P = 80.5442, K_I = 15.0211, K_D = 1.5969, \lambda = 0.2739$ and $\mu = 0.6863$. The step response of the closed-loop system with MGWO-FOPID controller is compared with ZN-PID and

the system without controller in Figure 5.3. Frequency response of the system with MGWO-FOPID controller is shown in Figure 5.4.

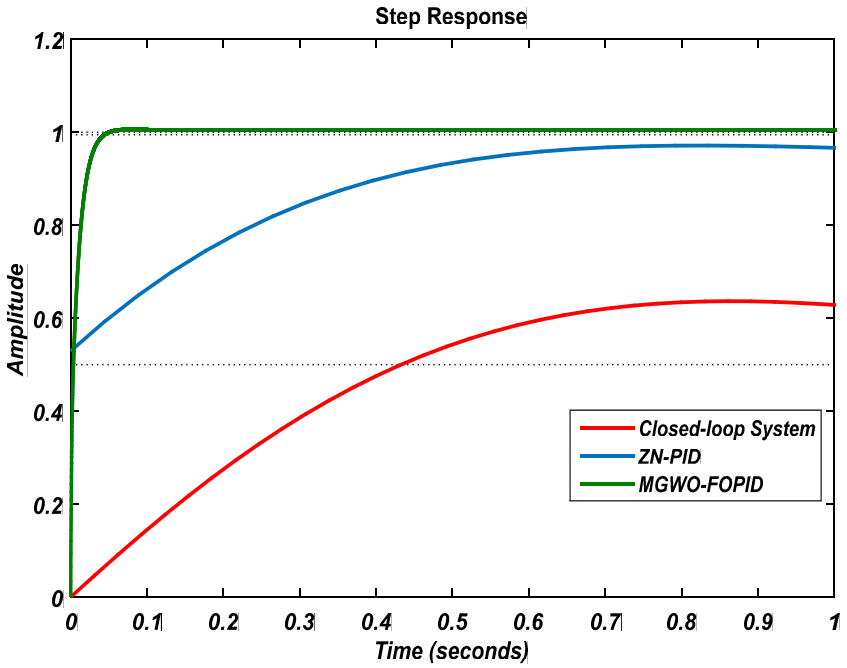

Fig. 5.3. Comparison of step responses of the closed-loop system with MGWO-FOPID, ZN-PID and the system without controller

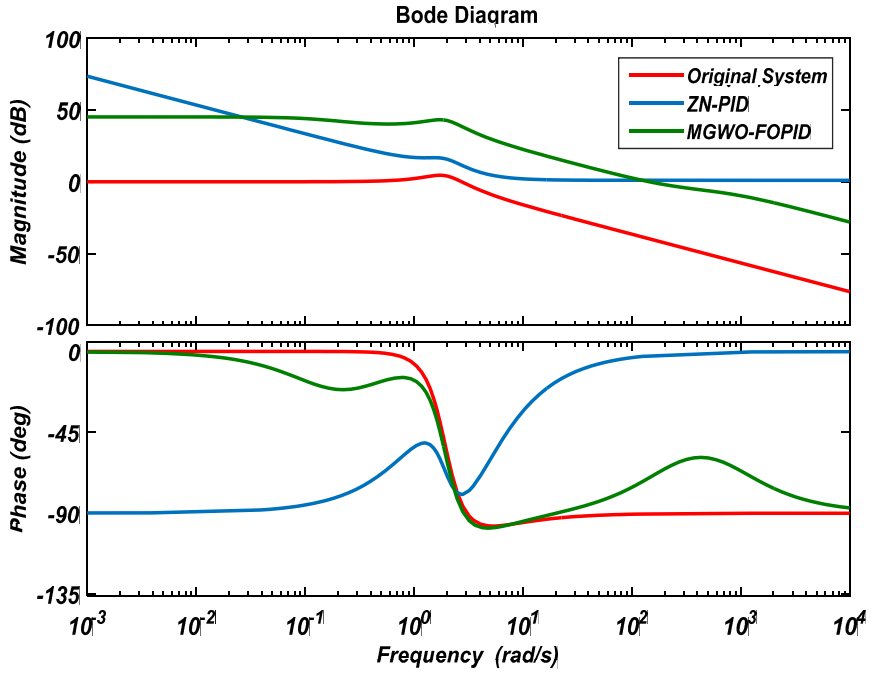

Fig. 5.4. Comparison of frequency response of the system without controller and the system with ZN-PID and MGWO-FOPID controller

Table 5.1 Comparison of performance characteristics of ZN-PID and MGWO-FOPID

Controller	Rise-time	Settling-time	Peak Overshoot	Gain Margin	Phase Margin
ZN-PID	0.5491	3.2580	0.9997	∞	∞
MGWO-FOPID	0.0188	0.0339	1.1442	∞	110

As shown in Figure 5.3, MGWO-FOPID controller present better performance than the ZN-PID controller both in time-domain and frequency domain specifications of the system. Performance characteristics of the plant with MGWO-FOPID is compared with the conventional ZN-PID controller in Table 5.1 which validates the effectiveness of the proposed algorithm over classical ZN-PID controller.

5.3.2 Design of an FOPID controller for systems with time delay

To validate the effectiveness of the MGWO-algorithm for time-delayed system FOPID controller is designed for both of the systems in section 3.3.2.

5.3.2.1 Second order system with time delay

The parameters of the FOPID controller optimized using MGWO-algorithm for the same system considered in section 3.3.2.1 are obtained as: $K_P = 8.3844, K_I = 2.8069, K_D = 5.4828, \lambda = 0.99352$ and $\mu = 0.85383$. The step response shown in Figure 5.5 depict the superiority of MGWO-FOPID controller as compares to the classical ZN-PID controller.

Performance characteristics of closed-loop time-delayed system with MGWO-FOPID controller is compared with the classical ZN-PID controller in Table 5.2. Here, we can observe that the MGWO-FOPID controller provides lesser settling time and negligible peak overshoot than the classical ZN-PID controller.

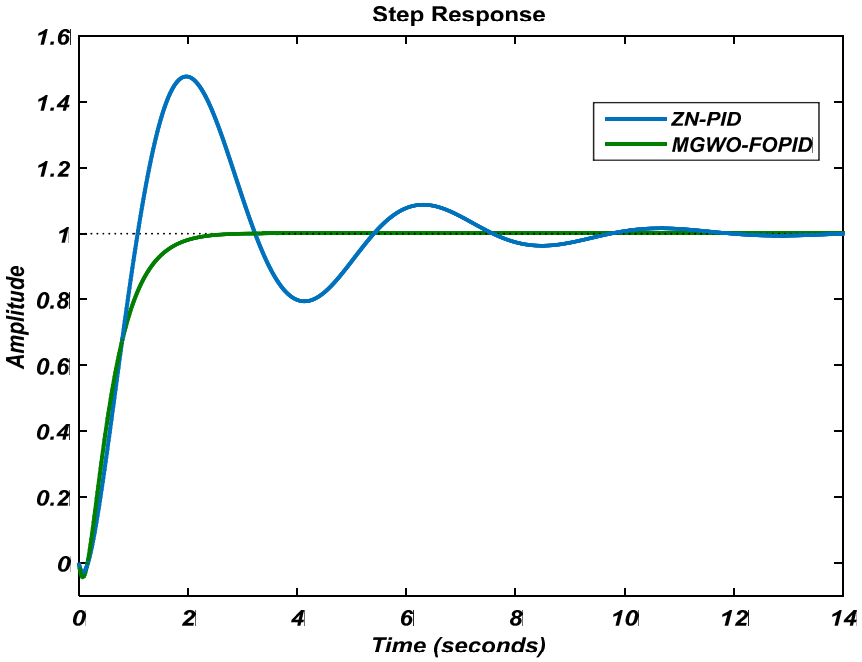

Fig. 5.5. Comparison of step response of the closed-loop time-delayed system with MGWO-FOPID and ZN-PID controller

Table 5.2 Comparison of performance characteristics of time-delayed system with ZN-PID and MGWO-FOPID controller

Controller	Rise-time	Settling-time	Peak Overshoot
ZN-PID	0.6871	9.2096	47.6680
MGWO-FOPID	1.0731	1.9603	0.0801

5.3.2.2 Non-minimum phase system with time delay

The parameters of the FOPID controller optimized using MGWO-algorithm for the system considered in section 3.3.2.2 are obtained as: $K_P = 0.0974, K_I = 0.7813, K_D = 3.5536, \lambda = 0.0033$ and $\mu = 0.4487$. The Figure 5.6 offer a favorable outcome of MGWO-FOPID controller than the classical ZN-PID controller.

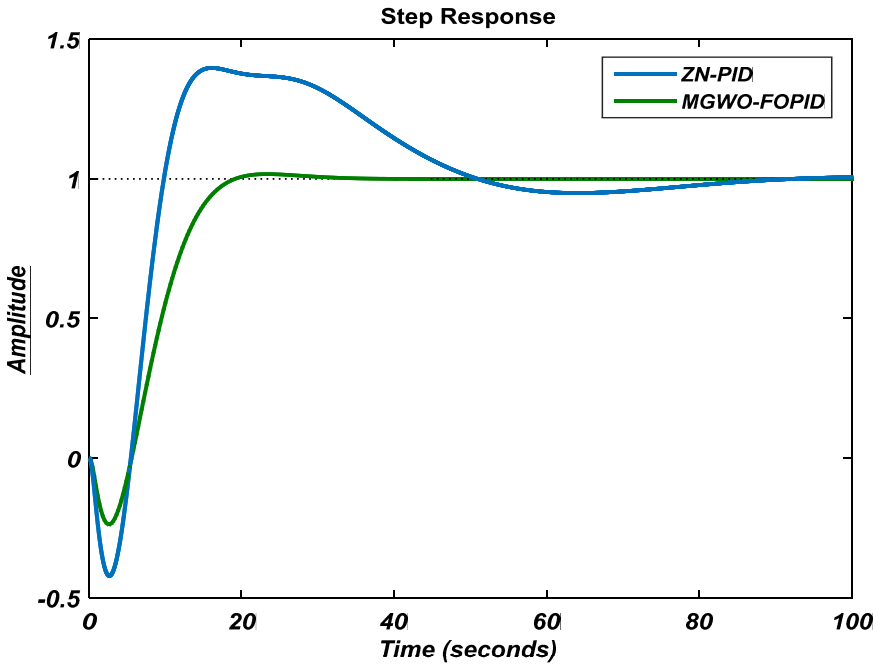

Fig. 5.6. Comparison of step response of the closed-loop NMP-system with ZN-PID and MGWO-FOPID controller

Table 5.3 Comparison of performance characteristics of NMP-system with ZN-PID and MGWO-FOPID

Controller	Rise-time	Settling-time	Peak Overshoot
ZN-PID	3.3664	77.4635	39.7292
MGWO-FOPID	8.5241	17.4682	1.7015

The performance characteristics of NMP-system is compared with the classical ZN-PID controller in Table 5.3 which shows the significant improvement in settling-time and maximum overshoot of the system. Although, the performance of the controller lags in case of rise-time of the system.

5.3.3 Design of an FOPID controller for magnetic levitation system

Consider the MLS from section 3.3.3. The optimized value of the controller parameters using MGWO-algorithm after 100 iterations are obtained as: $K_P = 72.9241, K_I = 20.2915, K_D = 73.9051, \lambda = 0.0582$ and $\mu = 1.8277$. The step response of the MLS with MGWO-FOPID is compared with the classical ZN-PID controller and TE-PID controller in Figure 5.7.

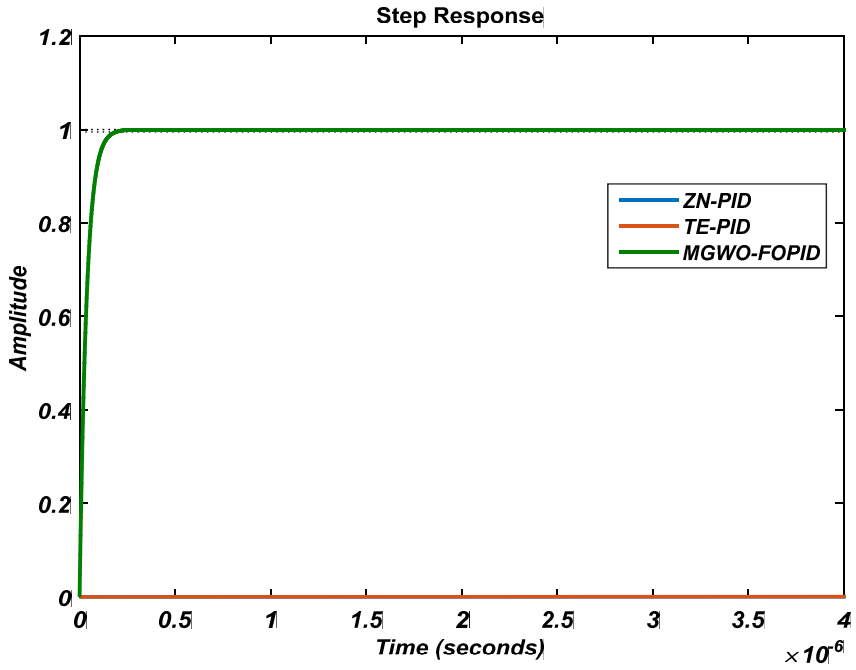

Fig. 5.7. Comparison of step response of the closed-loop MLS with ZN-PID, TE-PID and MGWO-FOPID controller

The performance characteristics of all three controllers are compared in Table 5.4 that validates the faster control action of the MGWO-FOPID controller over the classical PID controllers. It also reduces the peak overshoot of the MLS to a negligible value.

Table 5.4 Comparison of performance characteristics of MLS with ZN-PID, TE-PID and MGWO-FOPID controller

Controller	Rise-time	Settling-time	Peak Overshoot
ZN-PID	0.0096	0.503	37.6922
TE-PID	0.0068	0.2637	22.1133
MGWO-FOPID	$7.8089 * 10^{-8}$	$1.338 * 10^{-7}$	0.4096

5.3.4 Design of an FOPI Controller for a non-monotonic phase system

Consider the system in section 3.3.4. The optimized set of parameters of FOPI controller using MGWO (i.e. MGWO-FOPI) are as: $K_P = 715, K_I = 976.33, \lambda = 0.263$. Comparison of closed-loop system with MGWO-FOPI controller with classical ZN-PI is shown in Figure 5.8 which validate the faster control action of the proposed controller.

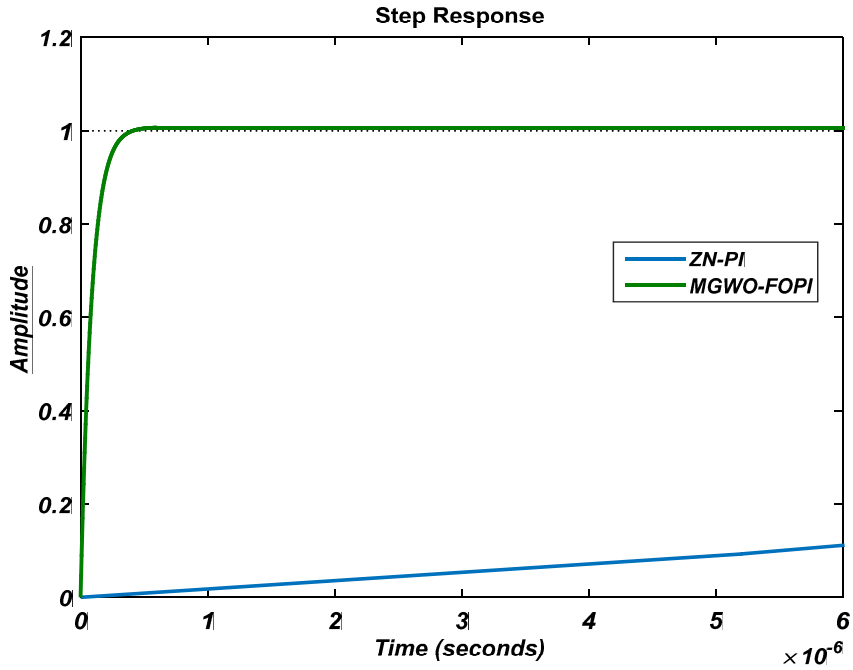

Fig. 5.8. Comparison of step response of the closed-loop DC-buck regulator with ZN-PI and GWO-FOPI controller

The frequency response is also compared in Figure 5.9 which show the improved gain of the system.

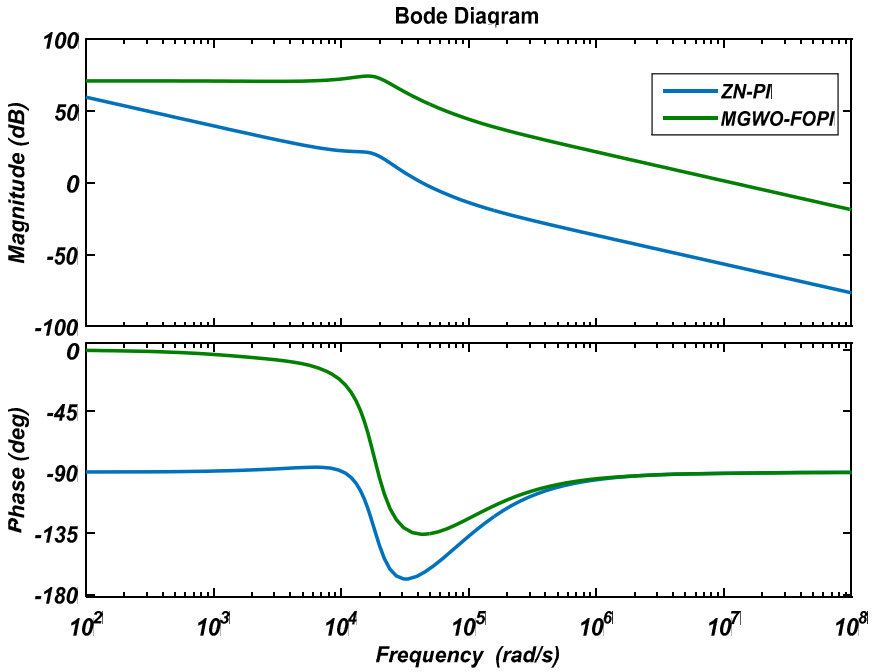

Fig. 5.9. Comparison of frequency response of the DC-buck regulator with ZN-PI and GWO-FOPI controller

Table 5.5: Comparison of performance characteristics of DC-buck regulator using ZN-PI and MGWO-FOPI controller

Controller	Rise-time	Settling-time	Peak Overshoot	Gain Margin	Phase Margin
ZN-PI	$2.75 * 10^{-5}$	$7.575 * 10^{-4}$	51.5141	∞	46.9
MGWO-FOPI	$1.8282 * 10^{-7}$	$3.0575 * 10^{-7}$	0.6896	∞	89.3

The performance characteristics compared in table 5.5 validates the faster control action and improved phase margin of the DC-buck regulator system with MGWO-FOPID controller over the ZN-PID controllers. Moreover, peak overshoot of the system reduced

to a negligible value. Hence, the MGWO-algorithm offer an efficient controller for DC-buck regulator system.

5.3.5 Design of an FOPID controller for a spherical tank system

The spherical tank system discussed in section 3.3.5 is considered here. The optimized set of parameters of FOPID controller optimized using MGWO-algorithms are obtained as: $K_P = 899.943, K_I = 689.999, K_D = 99.893, \lambda = 0.5378$ and $\mu = 0.49767$. The step response of the closed-loop STS with MGWO-FOPID is compared with that of the ZN-PID controller in Figure 5.10 which depict the faster response with negligible peak overshoot of the system.

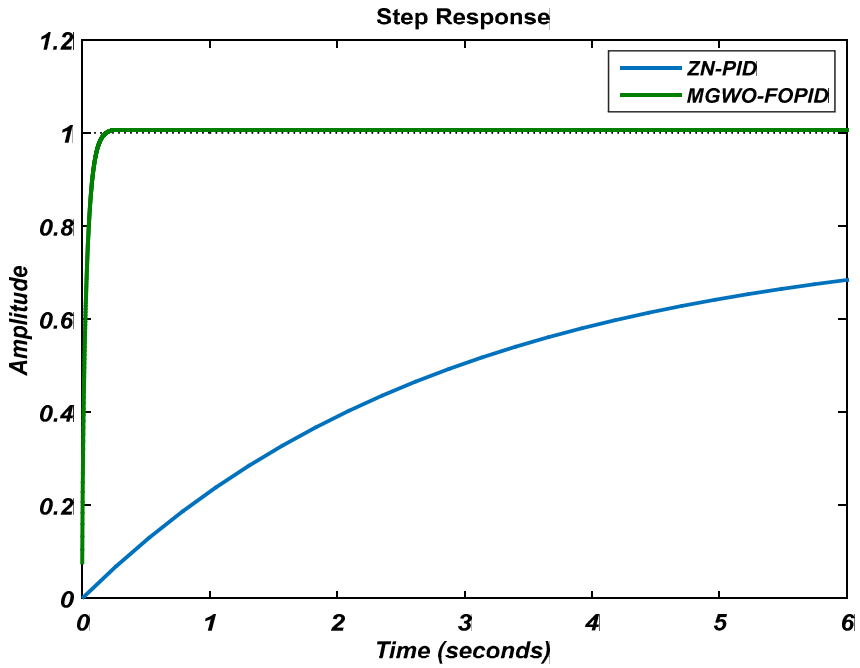

Fig. 5.10. Comparison of step response of the closed-loop STS with ZN-PID and GWO-FOPID controller

The performance characteristics of the STS with MGWO-FOPID is compared with ZN-PID controller in Table 5.6 which offer the significant improvement in rise-time,

settling-time and peak overshoot. Hence, the proposed algorithm present an efficient controller for the system.

Table 5.6 Comparison of performance characteristics of ZN-PID and NM-FOPID

Controller	Rise-time	Settling-time	Peak Overshoot
ZN-PID	84.644	193.0292	1.8564
MGWO-FOPID	0.0796	0.1383	0.5357

5.3.6 Design of an FOPID controller for AVR system

The AVR system in section 3.3.6 is considered here. The optimized values of the parameters of the FOPID controller using MGWO-algorithm are as: $K_P = 11.2902, K_I = 1.1035, K_D = 0.4155, \lambda = 0.8714$ and $\mu = 1.7281$. The step response of the closed-loop AVR system with MGWO-FOPID controller is compared with that of ZN-PID controller is in Figure 5.11. Here MGWO-FOPID controller present faster control action with zero peak overshoot for the AVR system.

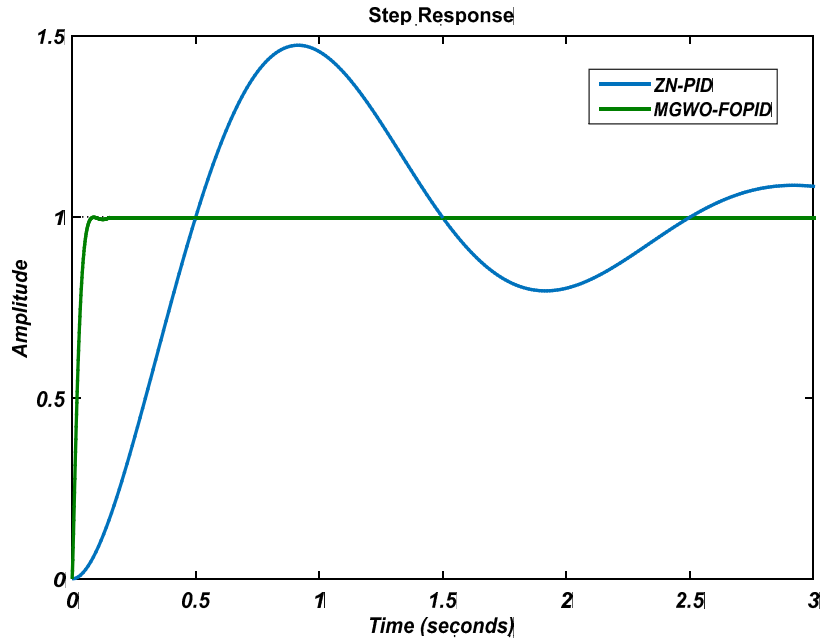

Fig. 5.11. Comparison of step response of the closed-loop AVR system with MGWO-FOPID controller and ZN-PID controller

Table 5.7 Comparison of performance characteristics of AVR system with ZN-PID and MGWO-FOPID controller for both values of β

Controller	Rise-time	Settling-time	Peak Overshoot	Gain Margin	Phase Margin
ZN-PID	0.3435	4.2656	47.3931	30.3	27.4
MGWO-FOPID	0.0427	0.0653	0	29.8	71

The performance characteristics of the AVR system with MGWO-FOPID controller are compared with the ZN-PID controller in Table 5.7. It is observed that the MGWO-FOPID controller enhance the overall performance of the AVR system. Robustness of the controller is validated in the next subsection.

5.3.7 Robustness analysis of MGWO-FOPID controller for AVR system:

In the present work robustness of the proposed MGWO-FOPID controller is validated by considering three different types of parameter uncertainties discussed section 4.7.

5.3.7.1 Uncertainty in amplifier

Assueme that the parameters of the amplifier change from its original value $K_A = 10, \tau_A = 0.1$ to $K_A = 14, \tau_A = 0.007$. The step response of the terminal voltage of both the original and the perturbed AVR system with MGWO-FOPID is shown in Figure 5.12. It is clear that the proposed algorithm provides a robust controller for uncertainty in amplifier parameters.

5.3.7.2 Uncertainty in exciter

Let the exciter parameters change from original value $K_E = 1, \tau_E = 0.4$ to $K_E = 1.2, \tau_E = 0.5$. The step response of both the original and the perturbed AVR system due to exciter uncertainties with MGWO-FOPID is shown in Figure 5.13.

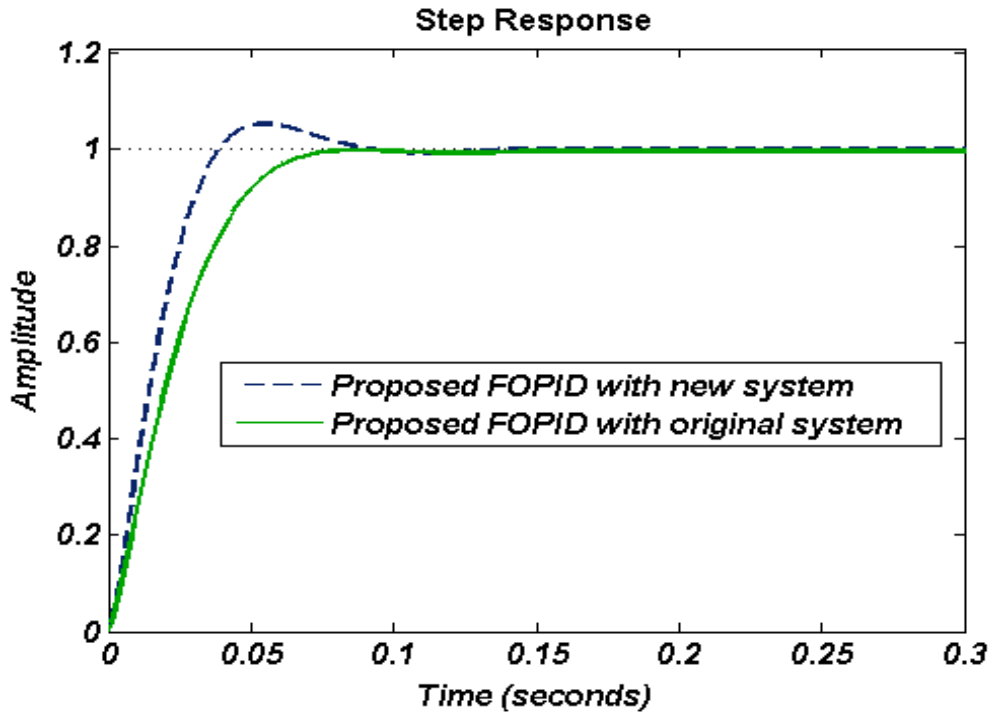

Fig. 5.12. Comparison of step response of original and altered AVR system due to uncertainty in amplifier

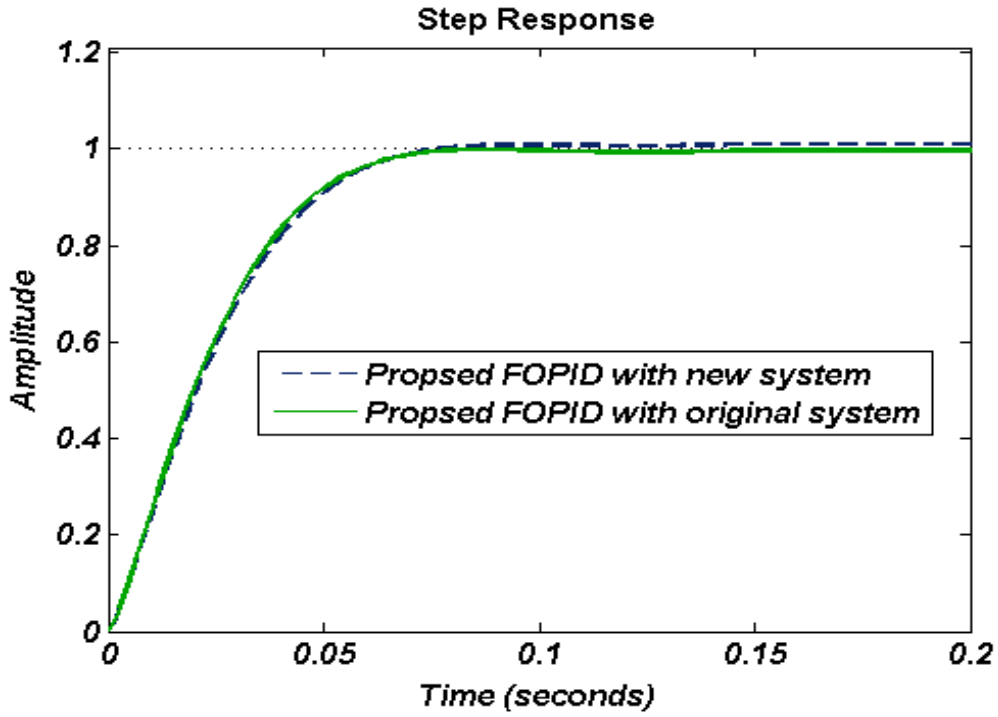

Fig. 5.13. Comparison of step response of original and altered AVR system due to uncertainty in exciter

5.3.7.3 Uncertainty in generator :

Allow the changes in generator parameter be from $K_G = 1, \tau_G = 1$ to $K_G = 0.7, \tau_G = 1.6$. The step response of both the original and the perturbed AVR system due to generator uncertainties with MGWO-FOPID is shown in Figure 5.14. The response shows the robust behavior of the proposed controller with uncertainty in generator parameters for AVR system.

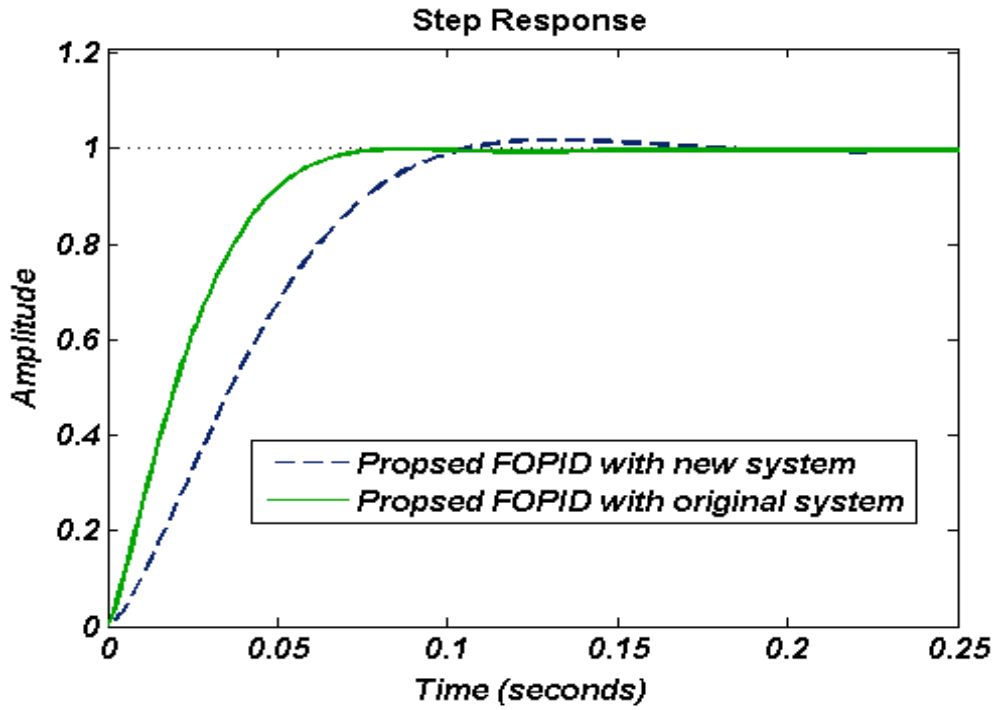

Fig. 5.14. Comparison of step response of original and altered AVR system due to uncertainty in generator

5.4 Summary

This chapter demonstrated an improved version of the GWO-algorithm for optimization of FOPID controller parameters. Performance of the algorithm is verified by designing the FOPID controller for different types of system. Effectiveness of the algorithm is validated by comparing the simulation results with ZN-PID controller. Moreover, the

performance of the proposed algorithm is tested for AVR system under uncertainty in amplifier, exciter and generator.

An extensive comparison of all the proposed algorithms for different plants in chapters 3, 4 and 5 is provided in the next chapter.